

## **ERL-BASED LEPTON-HADRON COLLIDERS: eRHIC AND LHeC**

F. Zimmermann, CERN, Geneva, Switzerland

### **Abstract**

Two hadron-ERL colliders are being proposed. The Large Hadron electron Collider (LHeC) plans to collide the high-energy protons and heavy ions in the Large Hadron Collider (LHC) at CERN with 60-GeV polarized electrons or positrons. The baseline scheme for this facility adds to the LHC a separate recirculating superconducting (SC) lepton linac with energy recovery, delivering a lepton current of 6.4mA. The electron-hadron collider project Erhic aims to collide polarized (and unpolarized) electrons with a current of 50 (220) mA and energies in the range 5–30 GeV with a variety of hadron beams— heavy ions as well as polarized light ions— stored in the existing Relativistic Heavy Ion Collider (RHIC) at BNL. The eRHIC electron beam will be generated in an energy recovery linac (ERL) installed inside the RHIC tunnel.



# ERL-BASED LEPTON-HADRON COLLIDERS: eRHIC AND LHeC

F. Zimmermann, CERN, Geneva, Switzerland

## Abstract

Two hadron-ERL colliders are being proposed. The Large Hadron electron Collider (LHeC) plans to collide the high-energy protons and heavy ions in the Large Hadron Collider (LHC) at CERN with 60-GeV polarized electrons or positrons. The baseline scheme for this facility adds to the LHC a separate recirculating superconducting (SC) lepton linac with energy recovery, delivering a lepton current of 6.4 mA. The electron-hadron collider project eRHIC aims to collide polarized (and unpolarized) electrons with a current of 50 (220) mA and energies in the range 5–30 GeV with a variety of hadron beams — heavy ions as well as polarized light ions — stored in the existing Relativistic Heavy Ion Collider (RHIC) at BNL. The eRHIC electron beam will be generated in an energy recovery linac (ERL) installed inside the RHIC tunnel.

## INTRODUCTION

The LHeC and eRHIC projects would involve one of the proton or ion beams of the LHC and RHIC, respectively. They, therefore, represent interesting possibilities for further efficient exploitation of the LHC and RHIC infrastructure investments. These and other (non-linac) lepton-hadron colliders, e.g. MEIC at TJNAF, are reviewed in [1].

For the LHeC [2], with 60-GeV lepton beam energy and using the 7 TeV proton (and few TeV / nucleon ion) beam, centre-of-mass collision (CM) energies in the TeV range are attained, significantly exceeding the CM energy of HERA, the first (ring-ring)  $ep$  collider built. The LHeC  $ep$  target luminosity is  $10^{33} \text{ cm}^{-2}\text{s}^{-1}$ . Extensions to  $10^{34} \text{ cm}^{-2}\text{s}^{-1}$  are being considered. In order to keep the power consumption of the LHeC facility at a realistic level, the total electrical power for the LHeC lepton branch has been limited to 100 MW. A Conceptual Design Report (CDR) has been published [3]. The LHeC physics program comprises precision QCD, electroweak physics, high parton densities, and new physics at high energy.

The LHeC CDR considered both ERL-ring and ring-ring options for the LHeC. Recently [4] the ERL-ring design was chosen as the baseline scheme for several reasons: (1) the installation of the ring-ring machine would interrupt the ongoing and planned LHC program as well as imply extended tunnel work and interference with the existing LHC, and (2) the development of a CW SC recirculating energy-recovery linac for LHeC would prepare for many possible future projects, e.g., for an International Linear Collider, for a neutrino factory, for a proton-driven plasma wake field accelerator, or for a muon collider. With some additional arcs, using 4 instead of 3 passes through the linacs, a machine like the LHeC ERL (without energy recovery) could also operate as Higgs factory  $\gamma\gamma$  collider [5].

The eRHIC [6] will collide 5–30 GeV polarized electron beams with 250–325 GeV polarized protons or 100–130 GeV / nucleon heavy-ion beams. The ultimate eRHIC luminosity per nucleon, achieved with lower hadron-beam emittances and with larger electron-beam currents than for the LHeC, is a factor 100–400 higher. In particular, eRHIC will employ a novel system of Coherent Electron Cooling (CEC) [7] to reduce the transverse and longitudinal emittances of the RHIC hadron beams, so that the normalized transverse emittances are about a factor 10 lower than those of the LHC. The enhanced space-charge tune shift requires a dedicated compensation by another electron beam [8]. For eRHIC, the total beam power loss, mainly due to synchrotron radiation, has been limited to about 10 MW. The ERL design offers a natural staging of the eRHIC facility where the beam energy is planned to be raised in steps as progressively additional SC cavities are installed and powered in the linac straights. The eRHIC physics program includes unraveling the origin of the proton spin, quantum phase space tomography of the nucleon, and the physics of strong color fields [9].

The luminosity of an ERL-ring collider can be written as

$$L = \frac{1}{4\pi e} \frac{N_{b,h}}{\varepsilon_h} \frac{1}{\beta_h^*} I_e H_{hg} H_D, \quad (1)$$

where  $e$  denotes the elementary charge,  $H_D$  the disruption enhancement factor ( $H_D \approx 1.3$  for  $e^-p/A$  and  $H_D \approx 0.3$  for  $e^+p/A$  collisions), and matched round colliding beams are considered. To obtain the maximum luminosity one aims for a large hadron bunch population  $N_{b,h}$ , a small geometric hadron-beam emittance  $\varepsilon$  (or large hadron-beam brightness  $N_{b,h}/\varepsilon_h$ ), a small hadron beam interaction-point (IP) beta function  $\beta_h^*$ , a high geometric overlap factor  $H_{hg}$  (head-on collision, and small lepton beam emittance), and, provided by the ERL, a large lepton beam current  $I_e$ .

Table 1 compares parameters for the two projects. In case of the LHC the geometric emittances for proton and ion beams are the same, and correspond to the values available in present operation. The projected eRHIC hadron beam emittances are determined from the expected performance of the CEC system and from imposing consistent requirements for the space-charge compensation system. As a result, in the case of eRHIC it is the normalized, not the geometric emittances, which is the same for heavy-ion and proton beams.

## LINACS, ARCS AND BEAM DYNAMICS

Both LHeC and eRHIC ERLs comprise two linacs. Their parameters are compared in Table 2. The LHeC linac is about 5 times longer and provides 4 times the energy gain, at comparable cavity voltage. The lower cavity filling factor for LHeC is partly due to the presence of about 100

Table 1: Collider parameters for eRHIC (ultimate) and LHeC (ultimate)

parameter [unit]	eRHIC		LHeC	
	$e^-$	$p, {}^{197}\text{Au}^{97+}$	$e^\pm$	$p, {}^{208}\text{Pb}^{82+}$
beam energy (/nucleon) [GeV]	15 (30)	325, 130	60	7000, 2760
bunch spacing [ns]	18	18	25, 100	25, 100
bunch intensity (nucleon) [ $10^{10}$ ]	2.4	40, 60	0.1, 0.4	17, 2.5
beam current [mA]	220 (12.6)	3330, 2000	6.4	860, 6
rms bunch length [mm]	2	49	0.6	75.5
polarization [%]	80	70, none	90 ( $e^+$ none)	none, none
normalized rms emittance [ $\mu\text{m}$ ]	5.8–57	0.2, 0.2	50	3.75, 1.5
geometric rms emittance [nm]	0.8	0.6, 1.4	0.43	0.50
IP beta function $\beta_{x,y}^*$ [m]	0.05	0.05	0.12	0.1
IP spot size [ $\mu\text{m}$ ]	6	6, 8	7	7
synchrotron tune $Q_s$	—	$4.6 \times 10^{-4}$	—	$1.9 \times 10^{-3}$
hadron beam-beam parameter		0.015		0.0001
lepton disruption parameter $D$		52, 22		6
crossing angle		0 effectively (crab crossing)		0 (detector-integrated dipole)
hourglass reduction factor $H_{hg}$		0.85		0.91
pinch enhancement factor $H_D$		1.2–1.3		1.35 (0.3 for $e^+$ )
CM energy [TeV]		140 (197), 88 (125)		1300, 810
luminosity / nucleon [ $10^{34} \text{ cm}^{-2}\text{s}^{-1}$ ]		14 (4), 8.4 (2.1)		0.1, 0.02

quadrupoles along the LHeC linac, whereas the eRHIC linac, of shorter length, does not include any focusing elements. No focusing in the linac implies larger linac beta functions and, thereby, a greater potential susceptibility to multi-pass beam break-up instabilities. For realizing the LHeC linac quadrupoles several options are being considered: electromagnets powered individually, electromagnets in clusters of 4 together with trims, and permanent magnets. The eRHIC will not use any cryomodules, but each eRHIC cavity will be an individual “cryounit” [10], designed for easy addition or removal. Estimated electrical power budgets for eRHIC and LHeC are dominated by the RF and cryo power required for the two SC linacs, as is illustrated in Table 3. The cryo power required and, therefore, also the size of the cryoplants are directly linked to the unloaded quality factor of the cavities,  $Q_0$ , since the cavity cryogenic RF loss at 1.8 K,  $U_{\text{loss}}$ , follows from  $U_{\text{loss}} = V_{\text{cav}}^2 / ((R/Q)Q_0)$ . The RF parameters, in addition to power needed for the control of microphonics (with 10 kW available per cavity in eRHIC [10]), must take into account the beam energy loss due to synchrotron radiation. For the LHeC, with an arc-dipole bending radius of 764 m, an electron loses about 2 GeV over all arc passes (including the deceleration) to be compared with a maximum beam energy of 60 GeV. LHeC and eRHIC plan to install dedicated RF systems to compensate for this energy loss. For LHeC the highest compensating RF voltage required is 750 MeV for the energy loss at 60 GeV, for which a fundamental 721 MHz system is to be used. At lower energies higher-harmonic RF systems operating at 1.44 GHz can simultaneously compensate for energy losses experienced on the accelerating and decelerating arc passes at the same beam energy. For eRHIC at 30 GeV peak lepton energy, with a dipole bending radius of 234 m, the total energy loss

per electron due to synchrotron radiation is about 770 MeV over all arc passes; at 20 GeV it is only 150 MeV. A single double harmonic compensator at (almost) the highest energy delivering 389 MeV per passage compensates for the energy loss from synchrotron radiation and other, smaller effects like resistive wall and linac-cavity HOMs [11].

Table 2: Parameters for eRHIC and LHeC SC linacs

parameter [unit]	eRHIC	LHeC
number of linacs	2	2
length / linac [km]	0.2	1.0
injection energy [GeV]	0.6	0.5
energy gain / linac [GeV]	2.45	10.0
number of acceleration passes	6	3
max. final energy [GeV]	30	60
real-estate gradient [MV/m]	12.45	10.0
energy gain / cavity [MeV]	20.4	20.8
cells / cavity	5	5
cavities / cryomodule (/cryounit)	1	8
cryomodules (cryounits) / linac	120	60
cryomodule length [m]	(100)	15.6
cavities / linac	120	480
RF frequency [MHz]	703.8	721
cavity length [m]	1.065	1.04
$R/Q$ [linac $\Omega$ ]	506	570
$Q_0$ [ $10^{10}$ ]	4.0	2.5
power loss / cavity [W/cavity]	23.7	32
“W per W” (1.8 K to R.T.)	700	700
filling factor	0.64	0.50
length / GeV [m]	82	97
cryopower / linac [MW]	2	10

In hadron storage rings, the proton and ion revolution and RF frequencies vary as a function of beam energy and species. For the LHC at top energy, it is possible to operate

Table 3: Electrical power budget for eRHIC and LHeC

parameter [unit]	electrical power [MW]	
	eRHIC	LHeC
total main-linac cryopower	4	21
RF microphonics control	5	24
extra-RF power for SR losses	20	23
extra-RF cryopower	0.3	2
electron injector	2.6	6
arc magnets	11	3
total	~43	78

the ion beams with the same RF frequency and harmonic number as the protons — a feature which will already be exploited for the first LHC  $p$ - $Pb$  collision run in early 2013. This means that the LHeC electron linac frequency can be held constant. In any case small electron path length changes are easily accomplished in the LHeC ERL with the help of dogleg-pairs downstream of each spreader [3]. For eRHIC the hadron-beam frequency variation is more important, due to the lower energy and smaller circumference, and due to a wide range of hadron-beam energies. Changing the eRHIC proton beam energy from 250 GeV to 50 GeV would imply an electron circumference change of 66 cm, which exceeds the maximum range (15 cm) of the planned path-length insertion. The path length changes required are brought into the tolerable range by switching the electron “harmonic number,” with a change by one unit (out of 9024) being equivalent to a path length change by one ERL RF wavelength, or 42.6 cm.

The lattice of the 6-passes for the eRHIC ERL arcs is based on low-emittance near-isochronous arc modules [12], supporting perfect isochronicity of complete paths. The standard building block is 35 m long, and contains 7 dipoles and 9 quadrupoles. The lattices for the 3 passes of the LHeC ERL arcs are based on a flexible-momentum compaction (FMC) optics design [13]. The standard building block is 52 m long, and contains 4 quadrupoles and 2 (split into 10) dipoles. The values of the curly-H function  $\langle H \rangle$  and  $M_{56}$  are tailored as required by emittance dilution and isochronicity or beam-size conditions, respectively, for arcs of different energies, transiting from a quasi-isochronous optics yielding a small beam size for the two lowest energy arcs, to a TME-optics for the two arcs at highest energy [13]. At the ends of each linac the beams are directed into the appropriate energy-dependent arcs for recirculation. For this purpose at both eRHIC and LHeC the beams are separated vertically and the arc dipoles for successive passes are stacked on top of each other. The LHeC arc dipoles have a 25 mm gap and a maximum field of 0.264 T, at 60 GeV [3, 14]. The eRHIC arc dipoles have a much smaller gap of 5 mm and, at 30 GeV, a maximum field of 0.43 T. In view of the small gap and high beam current, resistive-wall wake fields and surface-roughness effects are under careful investigation for eRHIC.

Concerning multi-pass beam-break up (BBU) [15] in the recirculating linac, simulations demonstrate that for LHeC beam stability requires both damping ( $Q \approx 10^5$ ) and detun-

ing ( $\Delta f/f_{\text{rms}} \approx 0.1\%$ ) of the higher-order modes (HOMs) in the 721-MHz linac cavities [16]. For eRHIC assuming the HOMs of the “BNL3 cavity” design and an HOM rms frequency spread of 0.1–0.2% the simulated BBU threshold is higher than the 50-mA design current [17]. If needed, for both eRHIC and LHeC the threshold of the transverse ERL-type beam-break up is substantially increased thanks to the natural chromaticity of the return arcs with a moderate (correlated) relative energy spread of order  $10^{-3}$  [18].

Collision of the leptons with the residual gas in the linac and arc beam pipes leads to the production of positive ions. With a CW beam, almost of these ions are trapped. Their presence adds additional focusing, modifying the optics, and can give rise to ion-driven transverse beam break up. The LHeC ERL circumference is chosen as 1/3 of the LHC circumference, so that ion clearing gaps can be introduced in the bunch train whose arrival times for successive passes coincide in the linacs and which, in addition, always correspond to the same partner hadron bunches in the LHC (so that the LHC would comprise hadron bunches which collide on every turn and some others which never collide). In these clearing gaps the ions drift away from the beam orbit. A good vacuum quality is also needed to further slow down the build up of a significant ion density during the bunch-train passages between successive clearing gaps. For the LHeC cold linacs partial gas pressures of  $10^{-11}$  hPa at 1.8 K are required at the position of the beam to render the residual fast beam-ion instability harmless. Pressures of, or below, this magnitude were achieved in the cold parts of LEP, HERA and LHC [3]. In the warm arcs of the LHeC a partial pressure below  $10^{-9}$  hPa should be sufficient [16]. Similar tolerances apply to eRHIC.

## INJECTORS

The LHeC electron injector is composed of a DC gun, where a photocathode is illuminated by a laser beam, generating a 7-mA polarized electron beam, and of a downstream linac bringing this electron beam to the 500-MeV injection energy of the ERL. After the linac, a bunch compressor system allows shortening the bunches to 1 ps. The transport efficiency to the IP as assumed to be 90%. A possible concern is the shape of the electron beam [19] and its effect on the hadron beam. The larger polarized-beam current of 50 mA required for eRHIC is provided either by means of a single large-size GaAs photocathode [20] or with a Gatling gun [21] combining beams from a large array of GaAs cathodes. An unpolarized SRF electron gun [22] could generate significantly higher beam current up to 220–250 mA CW. Table 4 summarises the electron beam parameters at the exit of the DC gun.

The 60-m long 600-MeV eRHIC injector linac is operated in energy recovery mode with the spent and fresh beams propagating in the same direction on a single passage. After deceleration the spent 50-mA beam is dumped with about 10 MeV energy (500 kW power). For the LHeC dumping the 6.4-mA spent beam at the ERL injection energy of 500 MeV amounts to 3 MW of power loss, which could be absorbed by a 3 m<sup>3</sup> water dump (0.5 m in diame-

Table 4: Source  $e^-$  beam parameters for eRHIC and LHeC.

parameter	eRHIC	LHeC
electrons / bunch [ $10^9$ ]	5.6, 24	1.1
charge / bunch [nC]	0.9, 3.8	0.18
rms bunch length [mm]	2	3–30
bunch spacing [ns]	18	25
average current [mA]	50, 220	7
bunch peak current [A]	50, 200	7–70
polarization	85–90%, none	> 90%

ter and 8 m long) with a  $3 \text{ m} \times 3 \text{ m} \times 10 \text{ m}$  long shielding. If the LHeC injector is configured for energy recovery as in the case of eRHIC, decelerating the spent beam to 10 MeV, the beam power at the dump decreases to 64 kW.

LHeC also assumes positron-hadron collisions. Obtaining the desired  $e^+$  rate is challenging. The source requirements may be relaxed by positron recycling, re-colliding, and cooling. A compact tri-ring scheme has been proposed for recooling the spent and recycled  $e^+$  [3, 23]. If, through these measures, the required positron intensity needed from the source is reduced by an order of magnitude, several concepts could provide the  $e^+$  intensity and the beam quality required, for example a Compton ring, a separate Compton ERL, or coherent pair production [3, 23].

## IR AND BEAM-BEAM EFFECTS

The eRHIC interaction-region (IR) design avoids high-energy X-rays from synchrotron radiation through a large crossing angle, complemented by crab cavities (for the hadron beam with about 23 MV crab RF voltage at a fundamental RF frequency around 200 MHz, plus two higher harmonic crab RF systems, and for the electron beam with a 1-MV crab voltage at 700 MHz [24]), and through arranging for zero or extremely low magnetic fields on the electron beam trajectory, over the last 130 m before the IP. Only 1.9 W of soft radiation propagates through the detector (from a 2.4-mT field). At the other extreme, the LHeC IR design achieves head-on collisions by means of two detector integrated dipoles surrounding the IP, each with a field of about 0.3 T and a length of about 9 m, leading to the emission of 48 kW of X-rays ( $1.78 \times 10^{18}$   $\gamma$ /s) with a critical energy of 718 keV. About 73% of this power will be absorbed by dedicated SR absorbers located in front of the final SC hadron-beam quadrupole at 10 m from the IP.

The final quadrupole for eRHIC, 5.475 m from the IP, is a combined function magnet with a dipole field of 2.23 T and 88 T/m gradient. The final quadrupole for LHeC is a “half quadrupole” with a low-field exit hole for the electron beam and for the second (non-colliding hadron) beam, while the colliding proton beam should experience a gradient of 187 T/m [14, 25]. Both eRHIC and LHeC final quadrupoles could be realized using  $\text{Nb}_3\text{Sn}$  SC magnet technology, presently under development in the frame of the LHC luminosity upgrade program.

For LHeC the hadron-beam beam-beam tune shift of  $\Delta Q \approx 10^{-4}$  is tiny — less than 1% of the LHC total p-p tune shift and of opposite sign — and, with  $36\sigma$  separation

at the first encounter provided by the near-IP dipole magnets, the effect of long-range collisions can be neglected. For eRHIC parasitic collisions are also unimportant, thanks to the 10-mrad crossing angle. Considering three collision points the maximum total beam-beam tune shift at eRHIC would be about 0.045, which is large, but consistent with experience at other colliders. A bigger concern is the hadron-beam emittance growth due to lepton-beam position jitter at the collision point. Extrapolating from Ref.[26] for LHeC the random orbit jitter from turn to turn should be less than  $0.08\sigma$  at the IP. For both LHeC and eRHIC the lepton beam is heavily disrupted during the collision, as is indicated by the large disruption parameters  $D \equiv N_{b,h} r_e \sigma_{z,h} / (\gamma_e \epsilon_h \beta_h)$  in Table 1. For LHeC the lepton beam emittance increases by about 15% with a proper matching of the extraction optics or by 180% if the exit optics does not take into account the optical effect of colliding with the proton beam. Similarly, the eRHIC lepton beam emittance grows by about a factor of 2 during the collision. The energy recovery path of the respective ERLs must accommodate these larger-emittance beams. For eRHIC the beam-beam kink instability is suppressed with a broad-band feedback system on the hadron beam [27]. At LHeC, with lower disruption parameter, much smaller hadron beam tune shift, and larger synchrotron tune the kink instability is not expected to occur [27].

## POLARIZATION

RHIC is the only polarized proton collider. In collisions at a beam energy of 250 GeV polarization at the level of 55% has been demonstrated and there are plans and means to push this polarization up to 70%. Proton polarization in the RHIC IPs is controlled by spin rotators. The heavy ions in RHIC, and all hadron beams in the LHC are unpolarized.

Polarized electron guns provide polarization at the 80–90% level. The direction of the electron spin can be flipped from one bunch to the next by changing the helicity of the gun laser photons. For eRHIC an economical way is chosen to maintain much of the source polarization and to orient it at the IP in the longitudinal direction. Namely there are no spin rotators and the spin is kept in the horizontal plane, rotating around the electron direction as a function of net bend angle and electron energy. In the proposed eRHIC layout the required orientation is obtained at RHIC Point 6 for collisions at discrete electron energies  $E_e = n \cdot 0.07216$  GeV, with  $n$  denoting an integer. Due to the finite energy spread the spin precession differs for different electrons in the beam. The effective polarization loss is given by the cosine of the spin vector spread angle; e.g. for an angle of  $30^{\text{deg}}$ , the effective polarization is about 86% of the initial beam polarization. For eRHIC, an rms energy spread of  $2 \times 10^{-4}$  (6 MeV) leads to a loss in polarization by about 5% for the 30-GeV electron beam. Applying the same approach as for eRHIC to the 60-GeV electron beam in the LHeC a relative rms energy spread of  $3 \times 10^{-4}$  (18 MeV) would cause about 10% polarization loss due to the spread of the spin vectors. Since this

does not satisfy the polarization requirement imposed by the physics program, for LHeC a different approach has been chosen. Namely, the LHeC lepton polarization is preserved by rotating it into the vertical direction before the beam gets accelerated to high energy. Since the spin vector is then aligned with the main bending magnetic field direction, this prevents the spread of the spin vector due to the momentum spread. RHIC type spin rotators [32, 33] are considered for the LHeC leptons. Besides being compact, they offer independent control of the spin vector orientation, as well as nearly energy independent spin rotation for the same magnetic field. The four helical dipoles are arranged in a similar fashion as for the RHIC spin rotator [3]. Each helical dipole is 15 m long and the helicity alternates between right hand to left hand. To align the spin vector of the polarized electrons in the longitudinal direction at the IP, the magnetic fields of the inner and outer pairs need to be 0.46 T and 0.37 T, respectively. About 0.31 MW of synchrotron radiation power is then emitted by the 60-GeV electron beam passing through these magnets [34]. An alternative HERA type spin rotator, consisting of a series of 8 dipoles, has also been studied. For the same total length of the system the required dipole fields are 0.46 T (H) and 0.56 T (V) with a total SR power of 0.39 MW [34].

## PLANS, OUTLOOK, AND THANKS

For the LHeC, in 2012 the R&D activities are focusing on preparation and on the exploration of possible collaborations with other research laboratories. This includes the choice of the preferred ERL RF frequency (721 MHz or 1.3 GHz). In 2013 the LHeC aims at the construction of a first SC IR model of the final quadrupole magnet with measurements on a short SC half-quadrupole magnet in 2014. A prototype of the IR beam pipes is also targeted for 2014. A final prototype RF cryostat including cavity and coupler is expected by 2015 [28]. The LHeC project will pursue the construction of a dedicated LHeC ERL test facility (Fig. 1), the design of which will be prepared over the next two years, with the goal of finalizing beam measurements by 2017. This test facility could later be converted into the LHeC injector, including energy recovery. In parallel, a proto-collaboration is scrutinizing the detector design [28]. The above steps would allow a project decision on the LHeC by the time when results from the 7-TeV beam energy operation of the LHC are expected to be available.

For eRHIC the list of needed accelerator R&D [29] includes the 50-mA CW polarized source, CEC, and testing multiple aspects of the SRF ERL technology in BNL's already existing R&D ERL [30]. A final prototype RF cryostat is envisioned for 2014. By 2015 a CEC proof-of-principle demonstration is expected at a RHIC-based experiment set up in collaboration with JLAB, Daresbury, BINP and Tech-X [31]. Other important eRHIC R&D focuses on prototyping small-gap magnets and vacuum chambers for the eRHIC arcs, with final prototype magnets expected by 2013. Also the space-charge compensation by an electron beam is part of the eRHIC R&D plan. Other

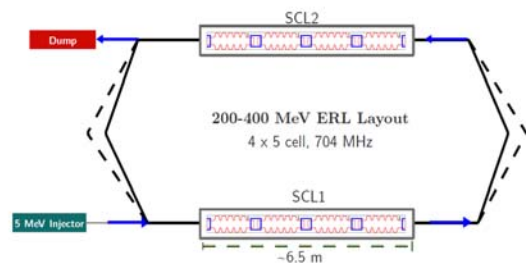


Figure 1: Schematic LHeC ERL test facility with two passes “up” and two passes “down”, using two SC RF prototype cryo modules (R. Calaga).

eRHIC R&D relates to studies with hadron beams in RHIC for the various eRHIC operation modes. Speculatively, the eRHIC operation could start around 2020, with collisions of 250 GeV protons and 5–10 GeV electrons, followed by 10-GeV steps in electron energy every 2–3 years.

I thank S. Belomestnykh, I. Ben-Zvi, V. Litvinenko and V. Ptitsyn for updated information about eRHIC, and M. Bai, A. Bogacz, O. Brüning, R. Calaga, E. Jensen, J. Jowett, M. Klein, L. Rinolfi, S. Russenschuck, D. Schulte, D. Tommasini, R. Tomas, and J. Tückmantel for many helpful discussions on the LHeC.

## REFERENCES

- [1] ICFA Beam Dynamics Newsletter No. 58, August 2012
- [2] LHeC web site: <http://cern.ch/lhec>
- [3] J.Phys.G: Nucl.Part.Phys. 39, 075001 (2012)
- [4] CERN-ECFA-NuPECC LHeC Workshop 14–15 June 2012
- [5] S.A. Bogacz et al., arXiv:1208.2827 (2012)
- [6] eRHIC web site: <http://www.bnl.gov/cad/eRhic>
- [7] V.N. Litvinenko, Y.S. Derbenev, PRL. 102, 114801 (2009)
- [8] V. Shiltsev et al., FERMILAB-CONF-9-152-APC
- [9] E. Aschenauer, eRHIC Review 2011
- [10] S. Belomestnykh et al., Proc. IPAC2012 Orleans, p. 2474
- [11] V. Ptitsyn, eRHIC Review 2011
- [12] D. Trbojevic et al., AIP CP 530 (2000) p. 333
- [13] A. Bogacz, et al, Proc. IPAC2011 San Sebastian, p. 1120
- [14] S. Russenschuck et al., IPAC2012 New Orleans, p. 1996
- [15] E. Pozdeyev, PRST-AB 8, 054401 (2005)
- [16] D. Schulte, private communication; and [3]
- [17] D. Kayran, eRHIC Review 2011
- [18] V. Litvinenko, PRST-AB 15, 074401 (2012)
- [19] Y. Saveliev, CERN ATS Seminar 5 Sept. 2012
- [20] E. Tsentalovich, 18th Int. Spin Physics Symp. (2008)
- [21] V. Litvinenko, CA/AP/417; X. Chang et al., PAC11, p. 1969
- [22] R. Calaga et al., Physica C 441 (2006), p. 159
- [23] F. Zimmermann et al., IPAC2012 New Orleans, p. 3108
- [24] V.N. Litvinenko, “Crab Crossing,” eRHIC Review 2011
- [25] R. Tomas et al., Proc. IPAC2011 San Sebastian, p. 2796
- [26] K. Ohmi et al, Proc. PAC07 Albuquerque, p. 1496
- [27] Y. Hao et al., Proc. IPAC12 New Orleans, p. 2017
- [28] O.S. Brüning et al., Proc. IPAC2012 New Orleans, p. 1999
- [29] V.N. Litvinenko et al., in Ref.[1], p. 52
- [30] I. Ben-Zvi et al., in Ref.[1], p. 151
- [31] V.N. Litvinenko et al., Proc. PAC2011, p. 2064
- [32] I. Alekseev et al., Nucl.Inst.Meth. A499, 392 (2003)
- [33] V. Ptitsyn, AGS/RHIC/SN No. 5 (1996)
- [34] M. Bai, “Spin Rotator” at [4]